Identification of Coronary Culprit Lesion in ST Elevation Myocardial Infarction by Using Deep Learning

LI-MING TSENG[1,2,4], CHENG-YEN CHUANG[3], SU-KIAT CHUA[3,4], AND VINCENT S. TSENG[2], (Fellow, IEEE)

[1]Department of Emergency Medicine, Shin Kong Wu Ho-Su Memorial Hospital, Taipei 11101, Taiwan
[2]Department of Computer Science, National Yang Ming Chiao Tung University, Hsinchu 30010, Taiwan
[3]Division of Cardiology, Department of Internal Medicine, Shin Kong Wu Ho-Su Memorial Hospital, Taipei 11101, Taiwan
[4]School of Medicine, College of Medicine, Fu Jen Catholic University, New Taipei 24205, Taiwan
CORRESPONDING AUTHOR: VINCENT S. TSENG (vtseng@cs.nycu.edu.tw)

ABSTRACT *Objective:* Early revascularization of the occluded coronary artery in patients with ST elevation myocardial infarction (STEMI) has been demonstrated to decrease mortality and morbidity. Currently, physicians rely on features of electrocardiograms (ECGs) to identify the most likely location of coronary arteries related to an infarct. We sought to predict these culprit arteries more accurately by using deep learning. *Methods:* A deep learning model with a convolutional neural network (CNN) that incorporated ECG signals was trained on 384 patients with STEMI who underwent primary percutaneous coronary intervention (PCI) at a medical center. The performances of various signal preprocessing methods (short-time Fourier transform [STFT] and continuous wavelet transform [CWT]) with different lengths of input ECG signals were compared. The sensitivity and specificity for predicting each infarct-related artery and the overall accuracy were evaluated. *Results:* ECG signal preprocessing with STFT achieved fair overall prediction accuracy (79.3%). The sensitivity and specificity for predicting the left anterior descending artery (LAD) as the culprit vessel were 85.7% and 88.4%, respectively. The sensitivity and specificity for predicting the left circumflex artery (LCX) were 37% and 99%, respectively, and the sensitivity and specificity for predicting the right coronary artery (RCA) were 88.4% and 82.4%, respectively. Using CWT (Morlet wavelet) for signal preprocessing resulted in better overall accuracy (83.7%) compared with STFT preprocessing. The sensitivity and specificity were 93.46% and 80.39% for LAD, 56% and 99.7% for LCX, and 85.9% and 92.9% for RCA, respectively. *Conclusion:* Our study demonstrated that deep learning with a CNN could facilitate the identification of the culprit coronary artery in patients with STEMI. Preprocessing ECG signals with CWT was demonstrated to be superior to doing so with STFT.

INDEX TERMS Convolutional neural network, electrocardiography, machine learning, percutaneous coronary intervention, STEMI.

Clinical and Translational Impact Statement—Deep learning may help identifying the infarct-related coronary artery in STEMI patients, speed up revascularization, and improve the clinical outcome.

I. INTRODUCTION

ACUTE coronary syndrome (ACS) is a syndrome due to decreased blood flow in one or more of the coronary arteries. Patients suffering from ACS have high risk of mortality and morbidity [1] To date, the diagnosis of ACS mostly depends on the symptoms of angina, elevation of serum cardiac enzymes, and the electrocardiogram (ECG). Among all the examinations, the ECG has become a valuable, rapid, inexpensive, and non-invasive tool assisting the clinician in the diagnosis, decision support of treatment strategy, monitoring treatment efficacy, and risk stratification in patients with ACS, especially ST elevation myocardial infarction (STEMI), which mandates immediate treatment and intervention [2] Primary

percutaneous coronary intervention (PPCI) is currently the preferred reperfusion strategy for treating patients with ST-elevation myocardial infarction (STEMI). Studies have demonstrated that shorter door-to-balloon or diagnosis to wire-crossing times can improve short-term and long-term outcomes in patients with STEMI [2], [3] Undertaking direct intervention targeting a coronary artery with a culprit lesion can hasten revascularization and reperfusion of the injured myocardium. Although rapid progress has been made in improving the analytical precision of cardiac troponin assays,[4] traditional electrocardiogram (ECG) interpretation remains a mainstay in the initial diagnosis of acute coronary syndrome in patients in whom it is suspected. This is because ST-elevation is the best readily available surrogate marker for detecting complete acute coronary artery occlusion. In patients with STEMI, ECGs are used widely to predict the location of culprit lesions,[5], [6], [7] and early and accurate identification of the infarct-related artery can facilitate prediction of the at-risk area of the myocardium and guide decision-making based on the urgency of revascularization.

Fiol et al. developed a simple algorithm by examining levels of ST-segment deviation in different leads to identify culprit lesions in patients with STEMI [8], [9] Tierala et al. [10] evaluated one ECG criteria for culprit artery prediction with the positive predictive value (PPV) of the LAD, LCX, and RCA as the IRA were 96%, 65%, and 92%, respectively. However, in their study, the ECGs were classified according to the criteria into LAD, RCA, LCX, and ''nonspecific'' groups prior to evaluation. In addition, patients with LBBB were also excluded. A significant portion of ECGs that met the indication of primary PCI might not be used in the study. In acute anterior myocardial infarction (AMI), ECGs are useful in predicting both left anterior descending (LAD) coronary artery occlusion and the site of occlusion in relation to the artery's major side branches [11] Fujii et al [12] focused on the left side of the heart and analyzed the ECGs of 435 patients with STEMI; they found that a large reciprocal ST-segment depression in the inferior leads and ST-segment depression in lead V5 are key ECG discoveries that, through comparison of the left main artery lesion with the LAD lesion, enable the determination of STEMI. Such discoveries have a positive predictive value of approximately 70%. However, identifying the culprit artery in patients with acute inferior STEMI is more challenging [7] Vives-Borrás et al [13] developed a three-step ECG algorithm (using the amplitudes of ST-segment deviation in different leads) to distinguish right coronary artery (RCA) and left circumflex artery (LCX) occlusion in patients with acute inferior STEMI. The algorithm achieved a sensitivity of 77%, specificity of 86%, and accuracy of 82%. Approximately 50% of patients with STEMI who are referred for primary PCI have significant stenosis in two or more major coronary arteries [14] The identification of culprit lesions in patients with STEMI with multivessel disease (MVD) is essential; the early results from the CULPRIT-SHOCK trial support a strategy of culprit-only revascularization during the index procedure

in patients with acute myocardial infarction complicated by cardiogenic shock [15] Noriega et al. sought to assess whether the presence of MVD modifies artery-related ST-segment changes in patients with acute coronary artery occlusion and described the subtle differences between artery-related ST-segment changes in the presence and absence of MVD [16] Occasionally, reciprocal changes may depress the ST segment and compete with the ST segment elevation resulting from AMI, [17] which increases the complexity of the interpretation and identification of culprit arteries.

In addition to traditional ECG interpretation, advanced mathematical methods have also been employed to develop coronary artery disease (CAD) diagnostic algorithms. Gregg et al. developed a classification system with logistic regression for prehospital 12-lead ECGs to identify culprit lesions; the system demonstrated a PPV of 100% for the LAD, 78% for the RCA, and 90% for the LCX [18] Gregg et al. also applied a similar multinomial logistic regression and developed a classifier to discriminate proximal RCA, middle-to-distal RCA, and LCX occlusion, [19] achieving a PPV of 64% to 78%. Machine learning methods have been applied to facilitate the identification of patients with CAD [20] Currently, the sensitivity of the automated interpretation of STEMI ranges from 34% to 95%, and the specificity ranges from 70% to 96% [21], [22], [23], [24], [25], [26] Artificial intelligence with neural network analysis was also introduced to detect CAD. Acharya et al. proposed a deep learning (a class of machine learning) algorithm with a convolutional neural network (CNN) structure comprising four convolutional layers, four max pooling layers, and three fully connected layers to diagnose CAD using 2-second- and 5-second-duration ECG signal segments [27] However, instead of culprit lesion detection, most of these studies focused on identification of the injured area during myocardial infarction when they mentioned of localization.

For culprit lesion detection in patients with STEMI, Mehta et al. applied artificial intelligence algorithms to identify culprit vessels in patients with STEMI by using 12-lead ECGs [28] and single-lead ECG segments, [29] achieving an overall accuracy of 79.4% and 77.4%, respectively. However, accuracy and sensitivity were inconsistent between leads and myocardial territories for the single-lead ECGs [30]

Artificial intelligence and machine learning have been used to analyze various biomedical signals. These technologies may enable the integration and interpretation of complex biomedical and health-care data in scenarios in which traditional statistical methods may not be sufficient[31] Previously, we evaluated the effectiveness of predicting the onset of ventricular fibrillation by using a CNN[32] In this work, a CNN is applied for identifying culprit lesions in patients with STEMI by using their ECGs.

II. METHODS AND PROCEDURES
A. PATIENTS
We reviewed the medical records of a single medical center for all emergency department (ED) patients for whom the

"STEMI protocol" was activated between 2016 and 2019. This retrospective study was approved by the institutional review board of the medical center. The aforementioned emergency physician–activated protocol operates 24/7 and has been proven to shorten the door-to-balloon time of revascularization[33] This protocol was activated for 652 patients over the course of the 4-year period. Diagnoses of STEMI were confirmed by an interventional cardiologist, and the patients received PPCI. Patients with the following conditions were excluded: those with unavailable digital ECG files (failed uploads from the ECG device or paper ECG for patients transferred from other hospitals), those with unacceptable ECG quality, those who personally refused PCI or whose family did so on their behalf, and those in an extremely critical condition that led to mortality before completing PCI.

All PCI reports and coronary angiography (CAG) images were reviewed by interventional cardiologists from the same hospital. Culprit lesions included in the PCI report were confirmed through CAG. If culprit lesions were not included in the PCI report, the cardiologist determined whether identification of the culprit lesion was possible (generally the culprit lesion was the coronary artery branch or one of the branches that received the intervention). Patients with incomplete or missing PCI reports in their electronic medical records were excluded from the study. Patients initially diagnosed with STEMI who had no CAG-confirmed evidence of critical coronary artery stenosis were also excluded. The diagnoses of these patients included coronary artery spasm, aortic dissection, small MI, acute (peri)myocarditis, and pulmonary embolism. Patients who died before revascularization and patients with three-vessel disease who were referred for a coronary artery bypass graft (CABG) were also excluded. An additional 17 patients were excluded because they had received PPCI for two or more coronary arteries and reviewers could not identify the infarct-related artery (IRA) through CAG or the CAG findings indicated that the cardiologist had directly sent the patient to receive a CABG. We then classified the culprit lesions as left main (LM), LAD, LCX, or RCA regardless of the occluded segment of the coronary artery. Only nine patients had LM as a culprit lesion; they were excluded from the study because the number of cases was insufficient for deep learning. Notably, a history of having received a CABG operation was not an exclusion criterion; however, four patients with such a history who had aortocoronary saphenous vein graft stenosis as the culprit lesion were excluded from this study.

Unlike in other studies, patients with a history of permanent pacemaker installation, previous MI, congenital heart disease, left ventricular hypertrophy, or a left bundle-branch block in the baseline ECG or with significant stenosis (>70%) in two or more major coronary arteries were not excluded from this study. Pacemaker rhythms were shown in the initial ECG of two patients in the LAD group, one in RCA and one in LCX groups. All these patients had right ventricle pacing lead placement, which resulted in LBBB morphology. All these patients' ECG met at least one of the modified Sgarbossa
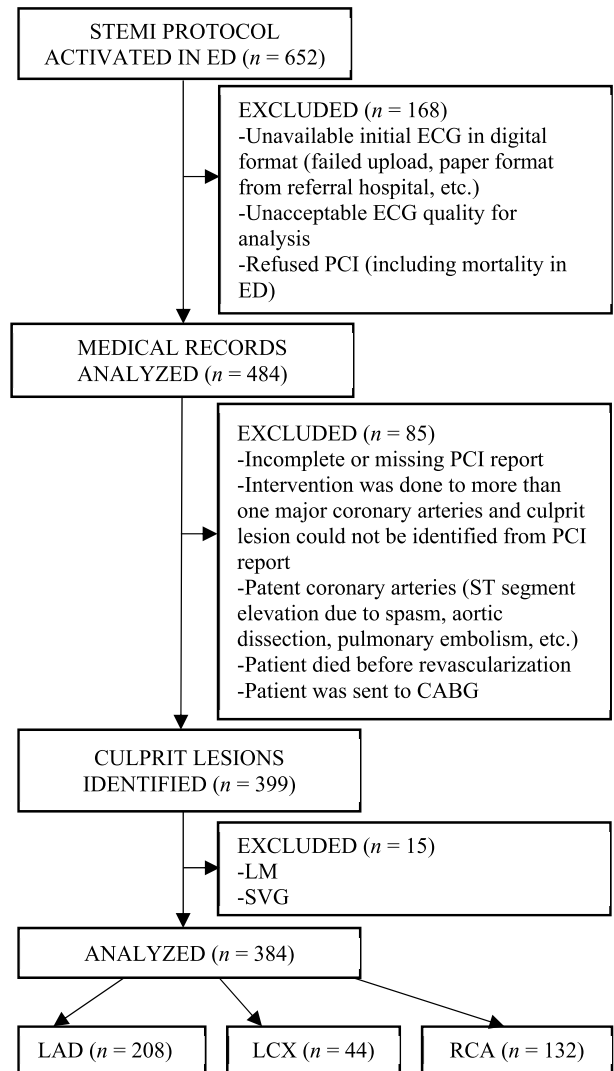

FIGURE 1. Diagram of the study and distribution of patients.

Criteria [34] which we also use to diagnose a STEMI in paced rhythm. And since LBBB patients were not excluded in our study, we've decided not to exclude these 4 patients.

Among included patients, 208 had LAD, 44 had LCX, and 132 had RCA as the culprit lesion. The ECGs of these patients were used to train and evaluate the machine learning model. The characteristics of patients at baseline are shown in Table 1. Of note, the average heart rates in the RCA and LCX groups are significantly slower than the LAD group, which is compatible with our current knowledge [35] [36] and can be explained by compromised perfusion to the sinoatrial (SA) and atrioventricular (AV) nodes or the Bezold-Jarisch reflex (increased vagal tone secondary to ischemia). The research was approved by the IRB of Shin Kong Wu Ho-Su Memorial Hospital on Sep 17, 2020 (protocol number: 20200809R).

B. WORKFLOW
The workflow of the methods proposed in this paper is illustrated in Figure 2. First, segments of ECG signals were extracted from the 12-lead ECGs of patients. For the original

TABLE 1. Characteristics of patients at baseline*.

| Characteristic	LAD as culprit (N=208)	LCX as culprit (N=44)	RCA as culprit (N=132)
Mean age, yr	60.8±12.3	58.6±13.7	60.1±14.1
Male sex, no. (%)	185 (88.9)	40 (90.9)	117 (88.6)
Diabetes, no. (%)	70 (33.7)	15 (34.1)	39 (29.5)
Chronic renal insufficiency, no. (%)	17 (8.2)	6 (13.6)	14 (10.6)
Previous myocardial infarction, no. (%)	13 (6.3)	7 (15.9)	10 (7.6)
Current smoker, no. (%)	89 (42.8)	22 (50)	67 (50.8)
Hypertension, no. (%)	121 (58.2)	21 (47.7)	69 (52.3)
Dyslipidemia, no. (%)	136 (65.4)	27 (61.4)	82 (62.1)
Previous PCI, no. (%)	25 (12.0)	7 (15.9)	15 (11.4)
Previous CABG, no. (%)	2 (1.0)	2 (4.5)	1 (0.8)
Previous stroke, no. (%)	11 (5.3)	3 (6.8)	3 (2.3)
PAOD, no. (%)	1 (0.5)	2 (4.5)	2 (1.5)
COPD, no. (%)	7 (3.4)	1 (2.3)	2 (1.5)
Heart rate (bpm)	86.3±21.5	78.8±26.9	72.1±18.6

*70% and 30% of patients were randomly assigned to training and test sets, respectively, in each epoch during model generation. PAOD, Peripheral arterial occlusion disease. COPD, Chronic obstructive pulmonary disease.

12-lead ECGs, 10 seconds of signals were recorded for all leads. The original ECG signals were acquired with Philips PageWriter TC70 cardiograph. High-pass filter with a cutoff of 0.5Hz and low-pass filter with a cutoff of 150Hz are applied by the cardiograph. The signals have sampling rate of 500Hz and are down-sampled to 250Hz in this study. From each ECG lead, we obtained a given number of ECG segments (all the 12 leads included) of fixed length, and the starting points of the segments were selected at random intervals. Compared to detecting specific waves prior to obtaining the ECG segments, random starting point saves time and computation cost, which makes more practical in future clinical device implementation. Similar method had been used in previous study [37] to classify cardiovascular diseases with CNN and accomplished high performance.
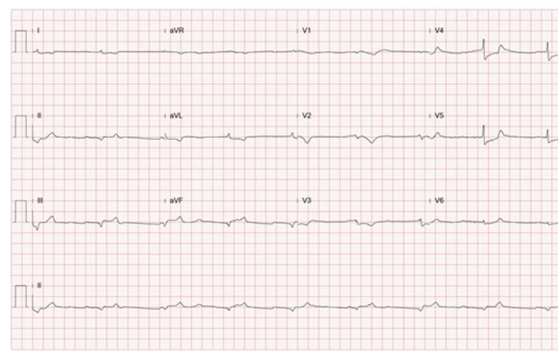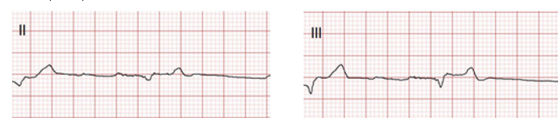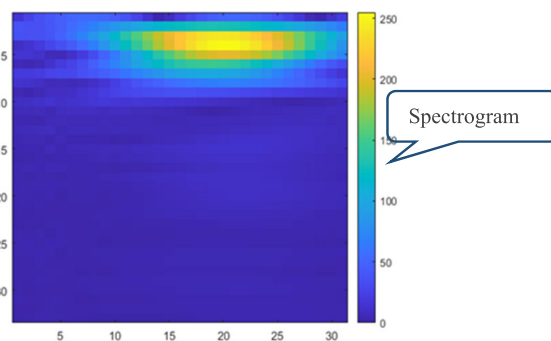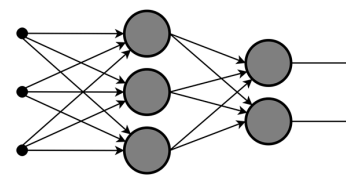

FIGURE 2. Workflow of identifying coronary culprit lesions with the proposed 2D CNN.

Second, the ECG segments underwent different methods of preprocessing. The purpose of the signal preprocessing was to obtain time–frequency analyses of the ECG signals to enable our proposed learning system to determine the culprit lesion. We considered different signal preprocessing methods. The details of these methods are discussed in the following subsection.

Third, the preprocessed ECG signals were fed into a CNN for training. The CNN performed linear and nonlinear

operations on the preprocessed ECG signals in multiple stages, and the output was used to determine the culprit lesion. The ECG signals used in the learning step were labeled, and by comparing the results of the CNN and the known labels, the weights of the CNN were adjusted to achieve more accurate classification (i.e., identification of the culprit lesion). The details of the CNN are provided in subsequent sections.

Finally, the performance of the various methods was evaluated using the structure and weights of the CNN. The evaluation was based on a test set containing ECG signals from different patients than those considered for training.

The patients for the training and test sets were randomly selected. The evaluation metrics included accuracy, sensitivity, and specificity.

C. ECG SIGNAL PREPROCESSING

ECG preprocessing was performed to extract time–frequency characteristics before deep learning. In this paper, we considered the following two methods:

1) SHORT-TIME FOURIER TRANSFORM (STFT)

Fourier transform is an essential signal analysis tool; it provides frequency spectrum and phase measurements. In the study of biomedical signals, frequency content variations are crucial. We applied the STFT technique, which introduces information regarding frequency changes in the spectral response with respect to time.

The STFT operation is briefly described as follows: A window is considered from the starting point of the signal, and discrete Fourier transform (DFT) is applied to the window. The window moves, maintaining a specified overlap with the previous window location, and DFT is performed again to obtain the frequency components of the second time interval. The operation is repeated until the signal ends. In this manner, we obtain a (sampled) spectrum with both frequency and time information. Regarding the window length, selecting a narrow window may result in poor, low-frequency resolution, whereas selecting a wide window produces poor time resolution at high frequencies. The inability to apply a time–frequency representation with perfect accuracy in both the time and frequency domains can be interpreted as an instance of the uncertainty principle. The STFT operation can be formulated as follows:

$$\text{STFT}\{x[n](m, \omega)\} \triangleq X(m, \omega) \sum_{n=-\infty}^{+\infty} x[n]w(n-m)e^{-i\omega n} \quad (1)$$

where $x[n]$ and $w[n]$ denote the signal and window sequences, respectively, ω is the frequency sampling point, and m is the time shift.

As with most standard applications, the STFT is performed on a computer using the fast Fourier transform (FFT). We then calculate the magnitude of the STFT results. After these operations are performed, the one-dimensional (1D) ECG signal becomes a two-dimensional (2D) time–frequency signal. Hamming window is used in the preprocessing,
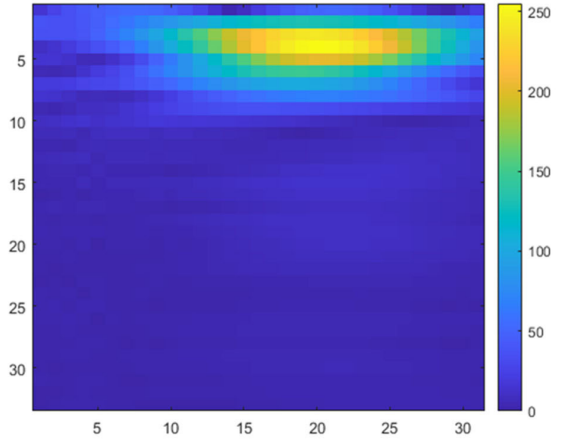

FIGURE 3. Example of STFT output of an ECG segment.

window length is 64, with overlap of 25%. An example of the magnitude of the STFT for an ECG segment is displayed in Figure 3, in which the x-axis represents the time domain and the y-axis represents the frequency domain. The ''parula'' colormap from MATLAB was used for visualization.

2) CONTINUOUS WAVELET TRANSFORM (CWT)

CWT is another popular method for time–frequency analysis of input signals. The CWT operation extracts the variation of signals with different scales that correspond to different frequencies. A wavelet of a smaller scale extracts the variation of signals faster within a shorter interval, whereas a wavelet of a larger scale extracts the variation of signals slower within a longer interval. The CWT operation for input signal x(t) can be described by the following formula:

$$X_w (a, b) = \frac{1}{|a|^{\frac{1}{2}}} \int_{-\infty}^{\infty} x(t)\varphi_0^* \left(\frac{t - b}{a} \right) dt \quad (2)$$

where φ_0 is the mother wavelet, whose complex conjugated, scaled, and shifted versions are used to analyze signals. Parameters a and b represent the scale and time shift, respectively. In this paper, we use a real-valued Morlet wavelet as our mother wavelet for the CWT method:

$$\varphi_0 (t) = e^{t^2/2} \cos 5t \quad (3)$$

Scales 1 to 32 are used in this study. An example of the CWT magnitude for an ECG segment is displayed in Figure 4, in which the x-axis represents the time domain and the y-axis represents the scale (frequency) domain.

The STFT and CWT transform a 1D ECG signal into a 2D plot. In addition, our raw ECG signals were obtained from 12 leads and became a third dimension of input for our learning system. For example, with the CWT method, the input dimensions were 125, 32, and 12 for time, scale, and leads, respectively.

D. DEEP LEARNING STRUCTURE

We designed a CNN for the learning structure. The CNN structure is displayed in Figure 5. The learning structure
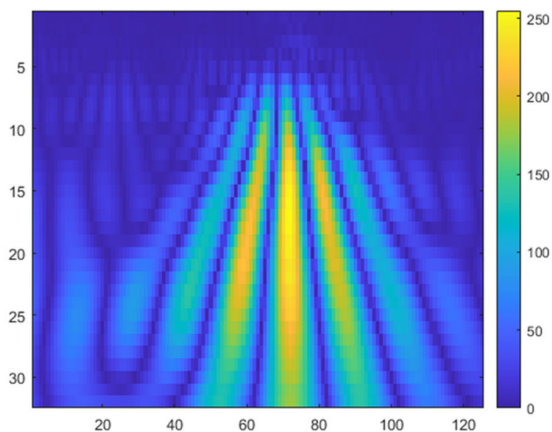
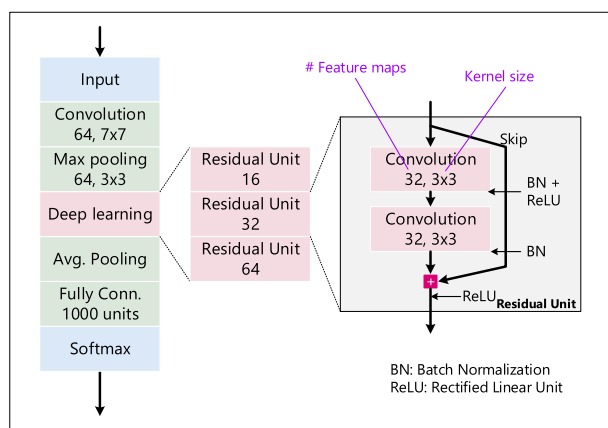**FIGURE 4.** Example of CWT output of an ECG segment.

FIGURE 5. CNN (ResNet) structure.

comprise a convolutional layer to perform the linear operation over the input, a multistage residual network which is the core of the CNN, and the output layer. Detailed explanations of the key enabling components are as follows:

1) ONE CONVOLUTION LAYER WITH POOLING

The convolution layers perform linear combinations of the input. In our approach, 2D convolution is performed, and nearby points in the time and frequency domains are correlated. One convolution layer comprises multiple feature maps, with each extracting a feature. Max pooling is applied after convolution to reduce the size of input to next step.

2) MULTISTAGE RESIDUAL NETWORK

In the main part of the CNN, we adopt a multistage residual network (ResNet),[38] which is developed as follows. The basic building blocks are residual units, each comprising two convolution layers with a skip layer that connects the input to output, and an activation layer (e.g., Rectified Linear Unit). ReLU serves as the default activation function when developing many CNNs because it overcomes the vanishing gradient problem, allowing models to learn faster and perform better. Batch normalization is also used to apply a transformation that maintains the mean output close to 0 and the

output standard deviation close to 1 to accelerate training. Multiple residual units with the same configurations (number of feature maps or filter size) are then cascaded to form a stage. The next stage has a similar structure; however, the configurations are different. In our design, the number of feature maps is doubled from one stage to the next. Three total stages are used.

3) OUTPUT LAYER

One fully connected layer is introduced after the ResNet and pooling layer. Average pooling is used instead of max pooling as in the original proposal of ResNet. All components are correlated to achieve full connection. The output from the fully connected layer is converted to probability values (range 0 to 1) using the *softmax* operation, and the results are used to determine if the predicted culprit lesion is compatible with the CAG.

The Python codes and samples of our patient ECGs (de-identified) can be found via the following link: https://drive.google.com/drive/folders/165cXGF6UvdKTy YR_YO6GrXI23Uo8OniN?usp=sharing.

E. EXPERIMENT EVALUATION

The patients with each culprit vessel category were divided into two sets: training and test. The ECG signal from each patient was segmented. The ECG segments for each patient were randomly assigned for use in a training or test set but not for use in both, even for different ECG segments from the same ECG. This ensured the independence of the training and test sets. The overall procedure of our experiment can be described as follows: approximately 70% and 30% of patients were assigned to a training and test set, respectively. For each patient, 100 ECG segments (all the 12 leads included) were extracted at random intervals between the segments. The extracted ECG segments were combined into batches of 128 segments. The training phase ran up to 100 epochs, and each epoch generated a learned model. A model generated by an early epoch (<100) was chosen if the test results (e.g., accuracy) were more favorable than those of later epochs.

To describe the performance of our proposed methods, we evaluated the following predictive metrics: overall accuracy; left versus right accuracy; and the sensitivity, specificity, and PPV for each culprit coronary artery. Since the majority of STEMI patients with RCA or LCX as the IRA had inferior MI, these patients were selected and the accuracy of prediction was evaluated. Different input ECG signal lengths and preprocessing methods were compared.

The performance of the criteria proposed by Tierala [10] using our database was also evaluated.

III. RESULTS

In total, 384 patients with STEMI were included. Among them, 208 had the LAD, 44 had the LCX, and 132 had the RCA as the culprit artery. No statistically significant differences were identified with respect to age, sex, history of diabetes mellitus, chronic renal insufficiency,

TABLE 2. Evaluation results of STFT method.

Duration	0.5s	1s	2s
Overall accuracy	69.92%	73.08%	79.31%
L vs. R accuracy	75.54%	75.31%	82%
LAD sensitivity	81.69%	77.46%	85.69%
LAD specificity	71.77%	88.39%	87.62%
LAD PPV	74.32%	86.96%	87.37%
LCX sensitivity	37%	3%	26.67%
LCX specificity	94.17%	99%	98.22%
LCX PPV	45.31%	28.13%	66.12%
RCA sensitivity	64.5%	88.4%	86.8%
RCA specificity	82.44%	67.13%	79%
RCA PPV	69.65%	62.70%	72.09%
RCA vs. LCX accuracy in inferior STEMI	70.6%	74.5%	72.7%

LAD, left anterior descending artery; LCX, left circumflex artery; RCA, right coronary artery

TABLE 3. Evaluation results of CWT method.

Duration	0.5s	1s	2s
Overall accuracy	73.69%	79.39%	83.69%
L vs. R accuracy	78.27%	82.42%	90.23%
LAD sensitivity	77.62%	85.62%	93.46%
LAD specificity	78.92%	77.69%	80.39%
LAD PPV	78.64%	79.33%	82.65%
LCX sensitivity	27%	56%	34%
LCX specificity	99.17%	99.74%	97.57%
LCX PPV	82.73%	96.55%	64.56%
RCA sensitivity	82.6%	78.3%	85.9%
RCA specificity	75.56%	85%	92.94%
RCA PPV	67.87%	76.54%	88.37%
RCA vs. LCX accuracy in inferior STEMI	74.8%	70.9%	66.8%

TABLE 4. Evaluation results of Tierala's criteria.

Overall accuracy	73.70%
L vs. R accuracy	82.58%
LAD sensitivity	94.09%
LAD specificity	89.41%
LAD PPV	90.67%
LCX sensitivity	34.15%
LCX specificity	91.11%
LCX PPV	33.33%
RCA sensitivity	72.87%
RCA specificity	88.11%
RCA PPV	77.69%

previous MI, smoking (current smoker), hypertension, dyslipidemia, stroke, peripheral arterial occlusive disease (PAOD), chronic obstructive pulmonary disease (COPD), or previous PCI and CABG between groups.

The evaluation results of the preprocessing methods are discussed in the following.

1) STFT METHOD
The evaluation results for the STFT method are provided in Table 2.

The overall accuracy improved with longer ECG segments. For example, the CNN achieved nearly 80% accuracy when using 2-second segments. The left versus right accuracy was higher than 80%. The sensitivity and specificity of the LAD and RCA cases were approximately 80%. Although the specificity of the LCX cases was good, the sensitivity was poor.

2) CWT (MORLET WAVELET) METHOD
The evaluation results for the CWT-based method are provided in Table 3.

The numerical results for the CWT-based method exhibited similar trends to those of the STFT-based method in terms of accuracy, sensitivity and specificity. However, the CWT-based method achieved higher (higher than 80%) overall accuracy.

3) TIERALA'S CRITERIA
The evaluation results for the Tierala's criteria are provided in Table 4.

IV. DISCUSSION
Our study demonstrated that with a properly designed neural network model and adequate subjects for training, the culprit coronary artery in patients with STEMI can be identified from ECGs.

The electrophysiological basis of ST-segment changes in MI can be explained by the electrical potential differences between normal and ischemic myocardial tissue (referred to as injury currents). The injury currents in transmural ischemia (which leads to STEMI) are directed from the infarcted area to the surrounding normal area of the heart, which results in ST-segment elevation in the corresponding leads. Thrombotic occlusion of more than one coronary artery is not rare; it occurred in up to 50% of patients in one autopsy series[39] One study suggested that complete revascularization could reduce the risk of cardiovascular death if performed either

during or after the index hospitalization ("staged" PCI)[40] However, timely treatment of the IRA and revascularization of the culprit lesion in primary PCI procedures remain the highest priorities. In patients with MVD, ECGs may reveal less ST-segment elevation, which increases the difficulty of ECG interpretation[16] Myocardial salvage is most likely to occur in early reperfusion; a strategy of performing ECG-guided PCI of the culprit coronary vessel followed by contralateral angiography may shorten the door-to-balloon time[41] Our study yielded a means for early identification of the IRA, better intervention planning, and potentially improved prognosis through the assistance of deep learning.

Reciprocal ST depression generally occurs in electrically opposite leads. For example, ST-segment elevation in the high lateral leads I and aVL typically produces reciprocal ST depression in lead III (inferior). This facilitates diagnosis in traditional ECG interpretation and may also provide key information for our neural network model. However, reciprocal change does not always occur. Therefore, ST depression in other leads should always be considered possible myocardial ischemia (subendocardial) of another area until proven otherwise. Because all 12 ECG leads were used in our model, the inclusion of depressed ST segments in other leads can also be used to train the model to improve the accuracy of culprit lesion prediction.

Ventricular premature contractions (VPCs) are not rarely seen in AMI patients. VPCs definitely affect the result of time-frequency analyses. STFT was also used in the analysis of APC and VPC [42] and CNN was used to localize the origins of VPC. [43] As we know, VPC is related to myocardial ischemia; the resulting information presented in the time-frequency analysis might also have some role the identification of the infarct-related artery. Thus, no special treatment was done to the VPCs in the original ECG signals in the study. Further studies focusing on the effect of VPCs may be conducted if sufficient cases can be enrolled.

Our study included 12 patients who had undergone return of spontaneous circulation (ROSC) and ST-segment elevation and who had survived to the completion of the PCI procedures. Most research has excluded these patients. The combined American College of Cardiology Foundation and American Heart Association in addition to the European Society of Cardiology have published STEMI guidelines recommending immediate coronary angiography and PCI, when indicated, for resuscitated out-of-hospital cardiac arrest (OHCA) patients with ST-segment elevation on their ECGs [44], [45], [46], [47] Acute coronary lesions have been identified in 70% to 80% of cases of OHCA patients who experienced ventricular fibrillation or pulseless ventricular tachycardia and were successfully resuscitated with sustained ROSC and ST-segment elevation or with a new left bundle-branch block on the surface ECG [48], [49] In our study, 11 of the 12 patients who had undergone ROSC had CAG-identified critical stenosis of at least one coronary artery. The overall accuracy of our model in identifying the culprit lesion in these patients was 49.6%, with

78.2% accuracy in predicting whether the culprit coronary artery was on the left (LAD or LCX) or right side (RCA). The sensitivity and specificity of identifying the LAD as the culprit lesion were both 79.6%, and the sensitivity and specificity for the RCA were 74% and 81%, respectively. Because only one patient had the LCX diagnosed as the culprit coronary artery, the sensitivity and specificity were 2% and 90.2%. More cases could not be included because most OHCA patients did not achieve sustained ROSC before receiving coronary angiography. Further inclusion of these patients would yield a more solid prediction model for identifying culprit coronary lesions to facilitate early revascularization.

One of the major contributions of this work is the preprocessing method. Our methods transformed 1D ECG signals into 2D time–frequency plots. To extract the time-varying features of the ECG signals, filters were applied to the ECG signals within moving windows. With the STFT-based method, the moving window size was fixed. With the CWT-based method, the moving window size was adjusted according to scale. As demonstrated by the results of the simulation, the CWT-based method outperformed the STFT-based method for most metrics. With the CWT-based method, more than 80% of the test cases were correctly classified, and when we only distinguished between the left and right vessels, the accuracy was higher than 90%. The advantage of the CWT-based method is its ability to extract different frequency components at different resolutions[50], [51] Higher-frequency features are extracted from more localized signals (i.e., smaller moving window sizes) because they are faster; lower-frequency features are slower, and they should be extracted using longer moving window sizes with wider-scale wavelets.

Another key design consideration is the choice of a mother wavelet for the CWT-based method. The Morlet wavelet is one of the most popular complex wavelets in ECG analysis; it has been demonstrated to have high frequency resolution [52]

We have also evaluated the performance of the criteria proposed by Tierala et al. [10] using our patient database. The PPV of the LAD, LCX, and RCA as the IRA were around 91%, 33%, and 78%, respectively. The overall accuracy was 74%, while the L vs. R accuracy was 83%. Compared to their traditional criteria, the CWT-based CNN model generally achieved better performance, which might help shorten the time to revascularization as mentioned previously.

This study has several limitations. First, the sensitivity in detecting the LCX as the culprit coronary artery was relatively low. This also occurs in traditional ECG interpretation. Patients with RCA or LCX artery occlusion can present with ST-segment elevation in leads II, III, and aVF. Several differential electrocardiographic criteria have been reported and clinically implemented [53] This difficulty in accurate prediction can be explained by individual variation in coronary artery anatomy, especially in the posterior descending artery. The posterior descending artery usually originates from the RCA. However, in some patients, it originates

from the LCX [54] Second, the performance of The CNN models tend to improve with longer ECG segments. The results of our study also showed this trend in LAD and RCA groups with both STFT and CWT methods. However, the LCX sensitivity and LCX PPV of the STFT-based method decrease remarkably with 1s ECG segment, and the LCX sensitivity and LCX PPV of the CWT-based method decrease with 2s ECG segment. This might be due to insufficient case numbers in LCX group which results in significant bias during random selection of the ECG segments during model training. As we know, it is relatively rare for LCX to be the culprit lesion in STEMI; further collection of the data might help solve this problem. Third, challenging situations may occur in which the ECG does not present typical diagnostic ST-segment elevations when the patient should be managed as a patient with STEMI according to an emerging consensus on "STEMI equivalents." For example, the de Winter pattern can be observed in approximately 2% of acute LAD occlusions and is often underrecognized by clinicians [55] Wellens syndrome [56] is another example in which critical stenosis of the LAD results in deeply inverted or biphasic T waves in V2-V3 without typical diagnostic ST-segment elevations. In some patients with critical left main coronary artery occlusion, ST-segment elevation may only be observed in lead aVR although widespread ST-segment horizontal depression presents in leads V4–V6. Posterolateral wall transmural infarction may present only in V1–V3 ST-segment depression on standard 12-lead ECGs, and the ST-segment elevation can only be detected with special ECGs using posterior leads V7–V9. Such patients do not meet the standard diagnostic criteria for STEMI and were not included in our study, although physicians and cardiologists have recently suggested that they should be managed as patients with STEMI. Further studies should focus on patients diagnosed with severe stenosis who underwent PCI when no diagnostic ST-segment elevation was observed in the initial ECG. If critical stenosis can be predicted in these patients, the proposed model of this study may provide a stronger and clearer indication for early intervention or primary PCI. Fourth, nonischemic causes of ST-segment elevation can occur: the presence of conduction defects and previous infarcts subvert the rules for identification,[57] hypercalcemia and hyperkalemia may cause ST-segment elevation in leads V1-V2, and acute pericarditis can interfere with ECG presentation [58] However, automated ECG interpretation with incorporated neural networks may also assist in differentiating these patients in the future.

V. CONCLUSION

This study demonstrated that deep learning with a CNN can aid in identifying culprit coronary arteries in patients with STEMI. Preprocessing ECG signals with CWT was demonstrated to be superior to doing so with conventional STFT. This is possibly due to the time-variant nature of ECG signals. The inclusion of more patients in the training set would further improve accuracy.

REFERENCES

[1] E. W. Tang, C.-K. Wong, and P. Herbison, "Global registry of acute coronary events (GRACE) hospital discharge risk score accurately predicts long-term mortality post acute coronary syndrome," *Amer. Heart J.*, vol. 153, no. 1, pp. 29–35, Jan. 2007, doi: 10.1016/j.ahj.2006.10.004.

[2] R. L. McNamara et al., "Effect of door-to-balloon time on mortality in patients with ST-segment elevation myocardial infarction," *J. Amer. College Cardiol.*, vol. 47, no. 11, pp. 2180–2186, Jun. 2006, doi: 10.1016/j.jacc.2005.12.072.

[3] B. Ibanez et al., "2017 ESC guidelines for the management of acute myocardial infarction in patients presenting with ST-segment elevation: The task force for the management of acute myocardial infarction in patients presenting with ST-segment elevation of the European society of cardiology (ESC)," *Eur. Heart J.*, vol. 39, no. 2, pp. 119–177, Jan. 2018, doi: 10.1093/eurheartj/ehx393.

[4] J. E. Hollander, M. Than, and C. Mueller, "State-of-the-art evaluation of emergency department patients presenting with potential acute coronary syndromes," *Circulation*, vol. 134, no. 7, pp. 547–564, Aug. 2016, doi: 10.1161/CIRCULATIONAHA.116.021886.

[5] M. J. Eskola et al., "Value of the 12-lead electrocardiogram to define the level of obstruction in acute anterior wall myocardial infarction: Correlation to coronary angiography and clinical outcome in the DANAMI-2 trial," *Int. J. Cardiol.*, vol. 131, no. 3, pp. 378–383, Jan. 2009, doi: 10.1016/j.ijcard.2007.10.035.

[6] T. Y. Kim, N. Alturk, N. Shaikh, G. Kelen, M. Salazar, and R. Grodman, "An electrocardiographic algorithm for the prediction of the culprit lesion site in acute anterior myocardial infarction," *Clin. Cardiol.*, vol. 22, no. 2, pp. 77–83, Feb. 1999, doi: 10.1002/clc.4960220205.

[7] M. Kosuge et al., "New electrocardiographic criteria for predicting the site of coronary artery occlusion in inferior wall acute myocardial infarction," *Amer. J. Cardiol.*, vol. 82, no. 11, pp. 1318–1322, Dec. 1998, doi: 10.1016/s0002-9149(98)00634-1.

[8] M. Fiol et al., "Evolving myocardial infarction with ST elevation: Ups and Downs of ST in different leads identifies the culprit artery and location of the occlusion," *Ann. Noninvasive Electrocardiol., Off. J. Int. Soc. Holter Noninvasive Electrocardiol.*, vol. 9, no. 2, p. 180, 2004.

[9] M. Almansori, P. Armstrong, Y. Fu, and P. Kaul, "Electrocardiographic identification of the culprit coronary artery in inferior wall ST elevation myocardial infarction," *Can. J. Cardiol.*, vol. 26, no. 6, pp. 293–296, Jun. 2010, doi: 10.1016/s0828-282x(10)70392-5.

[10] I. Tierala, K. C. Nikus, S. Sclarovsky, M. Syvänne, and M. Eskola, "Predicting the culprit artery in acute ST-elevation myocardial infarction and introducing a new algorithm to predict infarct-related artery in inferior ST-elevation myocardial infarction: Correlation with coronary anatomy in the HAAMU trial," *J. Electrocardiol.*, vol. 42, no. 2, pp. 120–127, Mar. 2009, doi: 10.1016/j.jelectrocard.2008.12.009.

[11] D. J. Engelen et al., "Value of the electrocardiogram in localizing the occlusion site in the left anterior descending coronary artery in acute anterior myocardial infarction," *J. Amer. College Cardiol.*, vol. 34, no. 2, pp. 389–395, Aug. 1999, doi: 10.1016/s0735-1097(99)00197-7.

[12] T. Fujii, M. Hasegawa, J. Miyamoto, and Y. Ikari, "Differences in initial electrocardiographic findings between ST-elevation myocardial infarction due to left main trunk and left anterior descending artery lesions," *Int. J. Emergency Med.*, vol. 12, no. 1, p. 12, Dec. 2019.

[13] M. Vives-Borras et al., "Electrocardiographic distinction of left circumflex and right coronary artery occlusion in patients with inferior acute myocardial infarction," *Amer. J. Cardiol.*, vol. 123, no. 7, pp. 1019–1025, 2019.

[14] D.-W. Park et al., "Extent, location, and clinical significance of non-infarct-related coronary artery disease among patients with ST-elevation myocardial infarction," *Jama*, vol. 312, no. 19, pp. 2019–2027, 2014.

[15] H. Thiele et al., "PCI strategies in patients with acute myocardial infarction and cardiogenic shock," *New England J. Med.*, vol. 377, no. 25, pp. 2419–2432, Dec. 2017, doi: 10.1056/NEJMoa1710261.

[16] F. J. Noriega et al., "Influence of the extent of coronary atherosclerotic disease on ST-segment changes induced by ST elevation myocardial infarction," *Amer. J. Cardiol.*, vol. 113, no. 5, pp. 757–764, Mar. 2014.

[17] K. Sasaki, M. Yotsukura, K. Sakata, H. Yoshino, and K. Ishikawa, "Relation of ST-segment changes in inferior leads during anterior wall acute myocardial infarction to length and occlusion site of the left anterior descending coronary artery," *Amer. J. Cardiol.*, vol. 87, no. 12, pp. 1340–1345, Jun. 2001, doi: 10.1016/s0002-9149(01)01549-1.

[18] R. E. Gregg and S. Babaeizadeh, "Detection of culprit coronary lesion location in pre-hospital 12-lead ECG," *J. Electrocardiol.*, vol. 47, no. 6, pp. 890–894, Nov. 2014.

[19] R. E. Gregg et al., "Automated discrimination of proximal right coronary artery occlusion from middle-to-distal right coronary artery occlusion and left circumflex occlusion in ST-elevation myocardial infarction," *J. Electrocardiol.*, vol. 45, no. 4, pp. 343–349, 2012.

[20] R. Alizadehsani et al., "Machine learning-based coronary artery disease diagnosis: A comprehensive review," *Comput. Biol. Med.*, vol. 111, Aug. 2019, Art. no. 103346.

[21] N. D. Brunetti et al., "Lower mortality with pre-hospital electrocardiogram triage by telemedicine support in high risk acute myocardial infarction treated with primary angioplasty: Preliminary data from the Bari-BAT public emergency medical service 118 registry," *Int. J. Cardiol.*, vol. 185, pp. 224–228, Apr. 2015, doi: 10.1016/j.ijcard.2015.03.138.

[22] J. L. Forberg et al., "In search of the best method to predict acute coronary syndrome using only the electrocardiogram from the emergency department," *J. Electrocardiol.*, vol. 42, no. 1, pp. 58–63, 2009.

[23] J. L. Garvey, J. Zegre-Hemsey, R. Gregg, and J. R. Studnek, "Electrocardiographic diagnosis of ST segment elevation myocardial infarction: An evaluation of three automated interpretation algorithms," *J. Electrocardiol.*, vol. 49, no. 5, pp. 728–732, Sep. 2016, doi: 10.1016/j.jelectrocard.2016.04.010.

[24] J. P. Ioannidis, D. Salem, P. W. Chew, and J. Lau, "Accuracy and clinical effect of out-of-hospital electrocardiography in the diagnosis of acute cardiac ischemia: A meta-analysis," *Ann. Emergency Med.*, vol. 37, no. 5, pp. 461–470, May 2001, doi: 10.1067/mem.2001.114904.

[25] P. J. Kudenchuk et al., "Utility of the prehospital electrocardiogram in diagnosing acute coronary syndromes: The myocardial infarction triage and intervention (MITI) project," *J. Amer. College Cardiol.*, vol. 32, no. 1, pp. 17–27, Jul. 1998, doi: 10.1016/s0735-1097(98)00175-2.

[26] K. Thygesen et al., "Third universal definition of myocardial infarction," *J. Amer. College Cardiol.*, vol. 60, no. 16, pp. 1581–1598, Oct. 2012, doi: 10.1016/j.jacc.2012.08.001.

[27] U. R. Acharya, H. Fujita, O. S. Lih, M. Adam, J. H. Tan, and C. K. Chua, "Automated detection of coronary artery disease using different durations of ECG segments with convolutional neural network," *Knowl.-Based Syst.*, vol. 132, pp. 62–71, Sep. 2017.

[28] S. Mehta et al., "P6421 can cardiologists rely on artificial intelligence to identify the culprit vessel in STEMI?" *Eur. Heart J.*, vol. 40, Oct. 2019, Art. no. ehz746.

[29] S. Mehta et al., "P6418 the continued proficiency of artificial intelligence for interpreting EKG: Single lead EKG for STEMI culprit lesion localization," *Eur. Heart J.*, vol. 40, Oct. 2019, Art. no. ehz746.

[30] S. Mehta et al., "Single lead for STEMI detection does not localize or identify culprit lesion," *J. Amer. College Cardiol.*, vol. 75, no. 11, p. 3624, 2020.

[31] K. Shameer, K. W. Johnson, B. S. Glicksberg, J. T. Dudley, and P. P. Sengupta, "Machine learning in cardiovascular medicine: Are we there yet?" *Heart*, vol. 104, no. 14, pp. 1156–1164, 2018.

[32] L.-M. Tseng and V. S. Tseng, "Predicting ventricular fibrillation through deep learning," *IEEE Access*, vol. 8, pp. 221886–221896, 2020, doi: 10.1109/ACCESS.2020.3042782.

[33] R. Parikh et al., "An emergency physician activated protocol, 'Code STEMI' reduces door-to-balloon time and length of stay of patients presenting with ST-segment elevation myocardial infarction," *Int. J. Clin. Pract.*, vol. 63, no. 3, pp. 398–406, Mar. 2009, doi: 10.1111/j.1742-1241.2008.01920.x.

[34] K. W. Dodd et al., "Electrocardiographic diagnosis of acute coronary occlusion myocardial infarction in ventricular paced rhythm using the modified Sgarbossa criteria," *Ann. Emerg. Med.*, vol. 78, no. 4, pp. 517–529, Oct. 2021, doi: 10.1016/j.annemergmed.2021.03.036.

[35] L. S. Dreifus, E. L. Michelson, and E. Kaplinsky, "Bradyarrhythmias: Clinical significance and management," *J. Amer. College Cardiol.*, vol. 1, no. 1, pp. 327–338, Jan. 1983, doi: 10.1016/s0735-1097(83)80033-3.

[36] C. V. Serrano, Jr., et al., "Sinus bradycardia as a predictor of right coronary artery occlusion in patients with inferior myocardial infarction," *Int. J. Cardiol.*, vol. 68, no. 1, pp. 75–82, Jan. 1999, PMID: 10077404, doi: 10.1016/s0167-5273(98)00344-1.

[37] H. Dai, H.-G. Hwang, and V. S. Tseng, "Convolutional neural network based automatic screening tool for cardiovascular diseases using different intervals of ECG signals," *Comput. Methods Programs Biomed.*, vol. 203, May 2021, Art. no. 106035, doi: 10.1016/j.cmpb.2021.106035.

[38] K. He, X. Zhang, S. Ren, and J. Sun, "Deep residual learning for image recognition," in *Proc. IEEE Conf. Comput. Vis. Pattern Recognit. (CVPR)*, Jun. 2016, pp. 770–778.

[39] M. J. Davies and A. Thomas, "Thrombosis and acute coronary-artery lesions in sudden cardiac ischemic death," *New England J. Med.*, vol. 310, no. 18, pp. 1137–1140, May 1984, doi: 10.1056/NEJM198405033101801.

[40] S. R. Mehta et al., "Complete revascularization with multivessel PCI for myocardial infarction," *New England J. Med.*, vol. 381, no. 15, pp. 1411–1421, 2019.

[41] M. C. Dib et al., "Culprit-vessel percutaneous coronary intervention followed by contralateral angiography versus complete angiography in patients with ST-elevation myocardial infarction," *Texas Heart Inst. J.*, vol. 39, no. 3, pp. 359–364, 2012.

[42] C. Mateo and J. A. Talavera, "Analysis of atrial and ventricular premature contractions using the short time Fourier transform with the window size fixed in the frequency domain," *Biomed. Signal Process. Control*, vol. 69, Aug. 2021, Art. no. 102835, doi: 10.1016/j.bspc.2021.102835.

[43] T. Yang, L. Yu, Q. Jin, L. Wu, and B. He, "Localization of origins of premature ventricular contraction by means of convolutional neural network from 12-lead ECG," *IEEE Trans. Biomed. Eng.*, vol. 65, no. 7, pp. 1662–1671, Jul. 2018, doi: 10.1109/TBME.2017.2756869.

[44] C. W. Callaway et al., "Part 8: Post-cardiac arrest care: 2015 American heart association guidelines update for cardiopulmonary resuscitation and emergency cardiovascular care," *Circulation*, vol. 132, pp. 465–482, Nov. 2015.

[45] P. T. O'Gara et al., "2013 ACCF/AHA guideline for the management of ST-elevation myocardial infarction: Executive summary: A report of the American college of cardiology foundation/American heart association task force on practice guidelines," *Circulation*, vol. 127, no. 4, pp. 529–555, Jan. 2013, doi: 10.1161/CIR.0b013e3182742c84.

[46] P. Steg et al., "Task force on the management of ST-segment elevation acute myocardial infarction of the European society of cardiology (ESC) ESC guidelines for the management of acute myocardial infarction in patients presenting with ST-segment elevation," *Eur. Heart J.*, vol. 33, no. 20, pp. 2569–2619, 2012.

[47] D. Yannopoulos et al., "The evolving role of the cardiac catheterization laboratory in the management of patients with out-of-hospital cardiac arrest: A scientific statement from the American heart association," *Circulation*, vol. 139, no. 12, pp. 530–552, 2019.

[48] S. Garcia et al., "Early access to the cardiac catheterization laboratory for patients resuscitated from cardiac arrest due to a shockable rhythm: The Minnesota resuscitation consortium twin cities unified protocol," *J. Amer. Heart Assoc.*, vol. 5, no. 1, 2016, Art. no. e002670.

[49] K. B. Kern et al., "Outcomes of comatose cardiac arrest survivors with and without ST-segment elevation myocardial infarction: Importance of coronary angiography," *JACC, Cardiovascular Intervent.*, vol. 8, no. 8, pp. 1031–1040, 2015.

[50] P. S. Addison, "Wavelet transforms and the ECG: A review," *Physiolog. Meas.*, vol. 26, no. 5, pp. 155–199, Oct. 2005, doi: 10.1088/0967-3334/26/5/R01.

[51] P. S. Addison, J. N. Watson, G. R. Clegg, M. Holzer, F. Sterz, and C. E. Robertson, "Evaluating arrhythmias in ECG signals using wavelet transforms," *IEEE Eng. Med. Biol. Mag.*, vol. 19, no. 5, pp. 9–104, Sep./Oct. 2000, doi: 10.1109/51.870237.

[52] A. M. Ciupe, R. V. Ciupa, A. I. Roman, and N. M. Roman, "Study of continuous wavelet transform used in ECG pre-diagnostic," in *Proc. E-Health Bioeng. Conf. (EHB)*, Nov. 2015, pp. 1–4.

[53] M. Fiol et al., "Value of electrocardiographic algorithm based on 'Ups and Downs' of ST in assessment of a culprit artery in evolving inferior wall acute myocardial infarction," *Amer. J. Cardiol.*, vol. 94, no. 6, pp. 709–714, 2004.

[54] M. J. Schlesinger, "Relation of anatomic pattern to pathologic conditions of the coronary arteries," *Arch Pathol.*, vol. 30, pp. 403–415, Jan. 1940.

[55] R. J. De Winter et al., "A new ECG sign of proximal LAD occlusion," *New England J. Med.*, vol. 359, no. 19, pp. 2071–2073, Nov. 2008, doi: 10.1056/NEJMc0804737.

[56] C. De Zwaan, F. W. Bär, and H. J. Wellens, "Characteristic electrocardiographic pattern indicating a critical stenosis high in left anterior descending coronary artery in patients admitted because of impending myocardial infarction," *Amer. Heart J.*, vol. 103, no. 4, pp. 730–736, Apr. 1982.

[57] F. M. Fesmire, R. F. Percy, J. B. Bardoner, D. R. Wharton, and F. B. Calhoun, "Usefulness of automated serial 12-lead ECG monitoring during the initial emergency department evaluation of patients with chest pain," *Ann. Emerg. Med.*, vol. 31, no. 1, pp. 3–11, Jan. 1998, doi: 10.1016/s0196-0644(98)70274-4.

[58] E. Durant and A. Singh, "ST elevation due to hypercalcemia," *Amer. J. Emergency Med.*, vol. 35, no. 7, p. 1033, Jul. 2017, doi: 10.1016/j.ajem.2017.02.005.